Acta Pharmaceutica Sinica B 2025;15(2):1171−1182

Chinese Pharmaceutical Association
Institute of Materia Medica, Chinese Academy of Medical Sciences

Acta Pharmaceutica Sinica B

www.elsevier.com/locate/apsb
www.sciencedirect.com

ORIGINAL ARTICLE

Engineering cellular dephosphorylation boosts (+)-borneol production in yeast

Haiyan Zhang[a,b,c], Peng Cai[b], Juan Guo[a], Jiaoqi Gao[b], Linfeng Xie[b], Ping Su[a], Xiaoxin Zhai[b], Baolong Jin[a], Guanghong Cui[a,*], Yongjin J. Zhou[b,*], Luqi Huang[a,c,*]

[a]*State Key Laboratory for Quality Ensurance and Sustainable Use of Dao-di Herbs, National Resource Centre for Chinese Materia Medica, China Academy of Chinese Medical Sciences, Beijing 100700, China*
[b]*Division of Biotechnology, Dalian Institute of Chemical Physics, Chinese Academy of Sciences, Dalian 116023, China*
[c]*Institute of Chinese Materia Medica, China Academy of Chinese Medical Sciences, Beijing 100700, China*

Received 15 October 2024; received in revised form 20 December 2024; accepted 24 December 2024

KEY WORDS

Borneol;
Monoterpene;
LPP1;
DPP1;
Nudix hydrolase;
Phosphatase

Abstract (+)-Borneol, the main component of "Natural Borneol" in the Chinese Pharmacopoeia, is a high-end spice and precious medicine. Plant extraction cannot meet the increasing demand for (+)-borneol, while microbial biosynthesis offers a sustainable supply route. However, its production was extremely low compared with other monoterpenes, even with extensively optimizing the mevalonate pathway. We found that the key challenge is the complex and unusual dephosphorylation reaction of bornyl diphosphate (BPP), which suffers the side-reaction and the competition from the cellular dephosphorylation process, especially lipid metabolism, thus limiting (+)-borneol synthesis. Here, we systematically optimized the dephosphorylation process by identifying, characterizing phosphatases, and balancing cellular dephosphorylation metabolism. For the first time, we identified two endogenous phosphatases and seven heterologous phosphatases, which significantly increased (+)-borneol production by up to 152%. By engineering BPP dephosphorylation and optimizing the MVA pathway, the production of (+)-borneol was increased by 33.8-fold, which enabled the production of 753 mg/L under fed-batch fermentation in shake flasks, so far the highest reported in the literature. This study showed that rewiring dephosphorylation metabolism was essential for high-level production of (+)-borneol in *Saccharomyces cerevisiae*, and balancing cellular dephosphorylation is also helpful for efficient biosynthesis of other terpenoids since all whose biosynthesis involves the dephosphorylation procedure.

*Corresponding authors.
E-mail addresses: guanghongcui@163.com (Guanghong Cui), zhouyongjin@dicp.ac.cn (Yongjin J. Zhou), huangluqi01@126.com (Luqi Huang).
Peer review under the responsibility of Chinese Pharmaceutical Association and Institute of Materia Medica, Chinese Academy of Medical Sciences.

https://doi.org/10.1016/j.apsb.2024.12.039

1. Introduction

(+)-Borneol, the main compound in Natural Borneol, is a valuable fragrant monoterpene used as a food flavoring and as a pharmaceutical[1-3] having analgesic, anti-inflammatory, and antimicrobial activities[4-7]. As one of the valuable and indispensable medical materials, (+)-borneol has been extensively used in traditional Chinese, Japanese, and Indian medicine for a long time[1,2]. In addition, the US Food and Drug Administration (FDA) has approved borneol as a flavoring agent. (+)-Borneol is prepared mainly by steam distillation extraction of fresh leaves of the *Cinnamomum* tree, which suffers from low yields (32.7%−81.8%)[8,9] and poses a threat to the sustainability of the plant species. Chemical synthesis is fraught with a high content (36%) of iso-borneol by-product[4], which is toxic and has other side effects[10].

Synthetic biology provides a sustainable answer for (+)-borneol production by engineering the biosynthesis pathways in microbes. The budding yeast *Saccharomyces cerevisiae*, a generally recognized as safe (GRAS) organism, has gained prominence as an ideal host for the production of high-value chemicals, such as artemisinic acid[11], cannabinoids[12], and alkaloids[13,14]. The strategies for efficient terpenoid synthesis in *S. cerevisiae* have been extensively studied, but the titer and yield of monoterpenes have always been inferior to that of diterpenes and sesquiterpenes[15-17], which are often attributed to the cytotoxicity and *in vivo* biotransformation of monoterpenes[18]. Although some acyclic or monocyclic monoterpenes, such as geraniol[19,20], citronellol[21] and ®-(+)-limonene[19], have been overproduced in *S. cerevisiae* at gram/liter levels, the production of (+)-borneol, a more complex bicyclic monoterpene, has remained low[22-24] (Table 1), even with optimizing the isoprenoid biosynthetic pathway and enhancing the supply of precursors and cofactors. As a result, effective strategies for boosting (+)-borneol production have puzzled researchers for a long time.

Engineering intracellular prenyl diphosphate may play an important role in terpene production, such as in the biosynthesis of α-santalene[25,26], geranylgeraniol[27], farnesol[28], and 11,20-dihydroxyferruginol[29], the endogenous phosphatases were deleted or overexpressed to increase their productions. Moreover, in the biosynthesis of borneol, bornyl diphosphate synthases (BPPS), which catalyzes the conversion of geranyl diphosphate (GPP) to bornyl diphosphate (BPP), exhibits an unusual characteristic compared with typical terpene synthase reactions (Supporting Information Fig. S1). Most terpene synthase reactions are terminated by deprotonation, resulting in the formation of alkenes or water-trapping and leading to alcohol formation[30-34]. However, in the catalytic cascade reaction of BPPS, bornyl cation is quenched by re-addition of inorganic diphosphate, resulting in BPP as the main product with minor by-products of (+)-α-pinene, (+)-camphene, (+)-limonene, terpinolene, and β-myrcene[31,35,36] Finally, phosphatases hydrolyze BPP to borneol. Although the endogenous phosphatase of yeast may mediate the dephosphorylation of BPP to borneol[23,24], this unusual dephosphorylation reaction may be a major obstacle to heterologous biosynthesis of borneol because the reaction would likely compete with cellular phosphorylation metabolism. Furthermore, the mechanism of endogenous phosphatase-mediated dephosphorylation of BPP remains unclear. Recent studies have shown that *EcNudJ*[22] and *WvNUDX24*[37] may be involved in the dephosphorylation of BPP, but whether they can effectively promote the production of (+)-borneol in yeast needs further evaluation. Thus, a comprehensive analysis of the mechanism of *de novo* synthesis of (+)-borneol in *S. cerevisiae* and identifying, characterizing phosphatases, and balancing cellular dephosphorylation metabolism is essential for enhancing (+)-borneol production.

Here, we first confirmed that BPP dephosphorization is the key factor in enhancing (+)-borneol production and reducing by-products. Thus, the endogenous phosphatases were systematically validated, and two phosphatases involved in (+)-borneol production were identified. We found that the Golgi apparatus serves as the primary site for (+)-borneol generation, where its membrane protein Lpp1 facilitates the conversion of BPP into (+)-borneol. Additionally, the mechanism of endogenous phosphatase competition between (+)-borneol synthesis and lipid metabolism was elucidated via lipidomic analysis and co-localization. To balance cellular dephosphorylation and boost (+)-borneol production, we identified and validated seven plant genetic elements through a combination of bioinformatic analysis and synthetic biology validation. Finally, by engineering BPP

Table 1 Borneol production in engineered microbes.

BPPS gene	Host	Cultivation condition	Shake flask titer (mg/L)	Bioreactor titer (mg/L)	Ref.
tLdBPPS^{S488T}	*E. coli*	YM9[a]	87.20	—[d]	22
tCbTPS1	*S. cerevisiae*	YPL[b]	2.89	—[d]	23
tBbTPS3	*S. cerevisiae*	YPL[b]	12.68	148.59	24
tSoBPPS	*S. cerevisiae*	YPD[c]	753	—[d]	This study

[a]YM9, containing 2 g/L yeast extract, 6 g/L Na_2HPO_4, 3 g/L KH_2PO_4, 0.5 g/L NaCl, 1 g/L NH_4Cl, 1 mmol/L $MgSO_4$, 0.1 mmol/L $CaCl_2$) and 10 g/L of glucose (unless otherwise stated).

[b]YPL, complex media containing 2% peptone, 1% yeast extract and 2% galactose.

[c]YPD, complex media containing 2% peptone, 1% yeast extract and 2% glucose.

[d]—, not applicable.

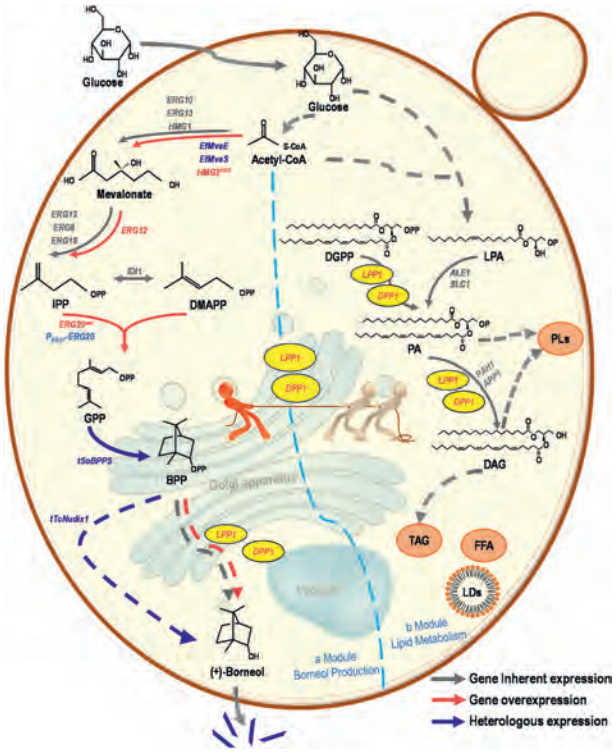

Figure 1 Schematic of engineering cellular dephosphorylation and mevalonate pathway to boost (+)-borneol production in yeast. A Module, optimizing the mevalonate pathway and engineering the dual pathway of BPP dephosphorylation enabled overproduction of (+)-borneol (753 mg/L). IPP, isopentenyl diphosphate; DMAPP, dimethylallyl diphosphate; GPP, geranyl diphosphate; BPP, bornyl diphosphate; *ERG10*, acetoacetyl-CoA thiolase; *ERG13*, 3-hydroxy-3-methylglutaryl-CoA synthase; *HMG1*, 3-hydroxy-3-methylglutaryl-CoA reductase; *EfMvaE*: acetyl-CoA acetyltransferase/HMG-CoA reductase; *EfMvaS*: HMG-CoA synthase; *HMG2*^{K6R}: HMG-CoA reductase 2 K6R mutant; *ERG12*, mevalonate kinase; *ERG8*, phosphomevalonate kinase; *ERG19*, mevalonate-5-diphosphate decarboxylase; *ID11*, isopentenyl diphosphate isomerase; *ERG20*, farnesyl diphosphate synthase; *ERG20*^{ww}: farnesyl diphosphate synthase mutant; *tSoBPPS*, truncated bornyl diphosphate synthase from *Salvia officinalis*; *LPP1*, lipid phosphate phosphatase from *Saccharomyces cerevisiae*; *DPP1*, diacylglycerol pyrophosphate (DGPP) phosphatase from *Saccharomyces cerevisiae*, *tTcNudix1*, truncated phosphohydrolase from *Tanacetum cinerariifolium.* B Module, schematic diagram of the lipid metabolism. DGPP, diacylglycerol diphosphate; LPA, lysophosphatidic Acid; PA, phosphatidate; DAG, diacylglycerol; TAG, triacylglycerol; FFA, fatty acid; PLs, phospholipids; LDs, lipid droplet. Genes shown in grey were endogenous yeast genes. Genes shown in red were overexpressed yeast gene. Genes shown in royal blue were heterologous. Gene shown in blue was downregulated gene.

dephosphorylation and optimizing the MVA pathway, we achieved a remarkable production of (+)-borneol (Fig. 1). This research not only fills a significant knowledge gap regarding the mechanism of *de novo* synthesis of (+)-borneol in *S. cerevisiae* but also lays a foundation for further exploration of efficient phosphatase with specific preference for BPP. The metabolic engineering strategies we used also provide a valuable understanding of the biosynthesis of other compounds that involve diphosphate precursors.

2. Materials and methods

2.1. Strains, medium and reagents

The yeast strains used in this study are listed in Supporting Information Table S1, and Supporting Information Fig. S2. Synthetic dropout (SD) solid medium (20 g/L glucose, 6.7 g/L yeast nitrogen base with $(NH_4)_2SO_4$ and without amino acids) was used for selection of recombinant strains. SD+5-FOA plates (20 g/L glucose, 6.7 g/L yeast nitrogen base with $(NH_4)_2SO_4$ and without amino acids,1 g/L 5-fluoroorotic acid, 20 mg/L histidine and uracil) were used for removing gRNA expression plasmids. Engineered strains for (+)-borneol production were cultivated in 100 mL flasks with 20 mL Delft minimal medium (pH 5.6) consisting of 5 g/L $(NH_4)_2SO_4$, 14.4 g/L KH_2PO_4, 0.5 g/L $MgSO_4 \cdot 7H_2O$, 20 g/L glucose, 2 mL/L trace metals (3.0 g/L $FeSO_4 \cdot 7H_2O$, 4.5 g/L $ZnSO_4 \cdot 7H_2O$, 4.5 g/L $CaCl_2 \cdot 2H_2O$, 1 g/L $MnCl_2 \cdot 4H_2O$, 300 mg/L $CoCl_2 \cdot 6H_2O$, 300 mg/L $CuSO_4 \cdot 5H_2O$, 400 mg/L $Na_2MoO_4 \cdot 2H_2O$, 1 g/L H_3BO_3, 100 mg/L KI, 19 g/L $Na_2EDTA \cdot 2H_2O$) and 1 mL/L vitamin solution (50 mg/L D-biotin, 1.0 g/L D-pantothenic acid hemicalcium salt, 1.0 g/L thiamine HCl, 1.0 g/L pyridoxin HCl, 1.0 g/L nicotinic acid, 0.2 g/L 4-aminobenzoic acid, 25 g/L m-inositol), supplemented with 20 mg/L histidine and uracil. *Escherichia coli* DH5α was used for plasmid amplification and cultivated in LB medium (10 g/L tryptone, 5 g/L yeast extract, and 10 g/L NaCl), in which 100 μg/mL ampicillin was used for plasmid maintenance. All plasmids are listed in Supporting Information Table S2.

Super Fidelity DNA polymerase, Taq DNA polymerase, and ClonExpress II One Step Cloning Kit were purchased from Vazyme Biotech, Nanjing, China. PrimeStar DNA polymerase was purchased from Takara Bio. DNA gel purification and plasmid extraction kits were purchased from Omega Bio-Tek, US. The standard (+)-borneol (CAS:464-43-7), α-pinene (CAS:80-56-8), (+)-camphene (CAS:79-92-5), β-myrcene (CAS:123-35-3), (+)-limonene (CAS:5989-27-5), and terpinolene (CAS:586-62-9) were purchased from Macklin.

2.2. Genetic manipulation

Primers were synthesized by Sangon Biotech (Shanghai, China) and listed in Supporting Information Table S3. Strain XC1 is a laboratory strain having a *CAS9* expression cassette integrated at the *X1−5* site in the *CEN.PK113−11C* strain and *GAL80* was deleted. Yeast DNA transformation was conducted using a chemical transformation method[38]. Target gene integration and deletion were performed using a CRISPR/Cas9-mediated gene editing system, and noncoding regions in the *S. cerevisiae* genome were chosen as integration sites to avoid affecting growth and metabolism[39]. All guide-RNAs (gRNAs) were designed by the CHOPCHOP web tool (http://chopchop.cbu.uib.no), and gRNA-expressing plasmids were constructed as described[40,41]. The donor was constructed with the one-step overlap extension PCR[42], in which endogenous genes, promoter, terminator, upstream and downstream homology arm were amplified from the genomic DNA of *CEN.PK113−11C*. Heterologous genes, such as *AvBPPS* from *Amomum villosum* (GenBank: MG763230), *LdBPPS* from *Lippia dulcis* (GenBank: MF133333), *SoBPPS* from *Salvia officinalis* (GenBank: AF051900) and *TcNudix1* from *Tanacetum cinerariifolium* (GenBank: MT126704) were codon-optimized for *S. cerevisiae* expression (Supporting Information Table S4) and synthesized by Sangon Biotech (Shanghai, China). The *CbTPS*1

gene from *Cinnamomum burmanni* (GenBank: MW196671) was amplified from plasmid pESC-LEU: *CbTPS1*[23].

2.3. Batch and fed-batch fermentation

The strains were first streaked on YPD plates and grown for 3−5 days. Then, single colonies were picked and precultured in 2.5 mL of YPD medium. After 16−20 h of cultivation, the strains were transferred into 20 mL of Delft minimal medium in 100 mL shake flasks for batch fermentation. The yeast cells were cultivated at 30 °C, 220 rpm for 72 h with an initial OD_{600} of 0.1. In addition, 10% (*v*/*v*) isopropyl myristate (IPM) was added to the culture to capture (+)-borneol. Fed-batch fermentation was conducted in 250 mL shake flasks with 50 mL Delft minimal medium or YPD medium, with an initial inoculation of OD_{600} = 0.4. The yeast cells were cultivated at 30 °C, 220 rpm, with 10% (*v*/*v*) IPM added for two-phase fermentation. During the fed-batch cultivation, residual glucose was quantified to determine the feeding rates. Cells were fed with 1−2 mL medium A (minimal medium) or medium B (modified YPD medium) when glucose was depleted. Medium A contained 500 g/L glucose solution, 25 g/L $(NH_4)_2SO_4$, 72 g/L KH_2PO_4, 2.5 g/L $MgSO_4 \cdot 7H_2O$, 10 × trace metal and 5 × vitamin solutions. Medium B contained 500 g/L glucose solution containing 50 g/L yeast extract and 100 g/L peptone. In addition, the pH was adjusted to 5.6 with the addition of 4 M KOH once a day. During the fed-batch process, samples were taken every 24 h to measure product titers and OD_{600}.

2.4. Extraction and quantification of (+)-borneol

After 72 h of cultivation, the biomass was measured from the OD_{600}, and the organic phase (10% IPM, which contains 100 mg/L (±)-camphor as an internal standard) was collected for product analysis. The organic phase was centrifuged at 13,000×*g* for 5 min to remove cellular debris and diluted with ethyl acetate to within an appropriate range. The (+)-borneol amounts were calculated by external standard calibration and corrected by using the internal standard (±)-camphor. GC−MS (Thermo Fisher Scientific) was used for qualitative analysis. Data were acquired in full-scan mode (*m*/*z* 50−650). The injection port temperature was 280 °C, and the oven temperature program was as follows: started at 80 °C for 2 min, ramped to 138 °C at a rate of 30 °C/min for 5 min, ramped to 150 °C at a rate of 5 °C/min for 2 min, and finally ramped to 320 °C at a rate of 50 °C/min and held for 5 min.

2.5. Fluorescence microscopy

To confirm tSoBpps subcellular localization, tSoBpps was fused to a green fluorescent protein (eGFP) at the N terminus or C terminus with a flexible linker GGGS; similarly, a red fluorescent protein (mPLUM) was fused to the N terminus or C terminus of Sec7[43] and Lpp1. The fusion cassettes were transformed into strain ZHY2. Colonies were cultivated in YPD medium for 18 h at 30 °C and 220 rpm. Cell cultures (5 μl) were dropped onto microscope slides and viewed with an EVOS M5000 microscope (Thermo Fisher Scientific). To confirm whether tSoBpps co-localized with vacuolar membrane protein Dpp1, the vacuolar membrane of strain ZHY47 was stained red with FM 4−64.

2.6. Lipidomic analysis

Lipidomic analysis was conducted with strains XC1 (wild-type), ZHY7 (without additional phosphatase), and ZHY73 (with additional phosphatase). Cells were cultivated in Delft minimal medium. Lipids were extracted and quantified as described[44] using (UPLC)-Q Exactive HF MS (Thermo Fisher Scientific). Relative contents of lipids were calculated by the ratio of peak area between lipids and internal standard per gDCW.

3. Results

3.1. Optimizing the mevalonate pathway

The limited availability of GPP and the strong competition for GPP by the endogenous sterol biosynthesis pathway essential for growth[45] makes it difficult to produce a pool of GPP sufficient for borneol synthesis. To address this issue, we overexpressed $ERG20^{ww}$ in the XC1 strain; $ERG20^{ww}$ encodes a mutant farnesyl diphosphate synthase (FPPS) that has a high efficiency of GPP synthesis. In the same strain, we co-expressed $HMG2^{K6R46,47}$, which encodes an HMG-CoA mutant that is known to stabilize the protein from protein degradation. In addition, we replaced the promoter of the endogenous *ERG20* with the *ERG7* promoter to reduce the GPP consumption by FPP synthesis[21], resulting in strain ZHY2 (Fig. 2A). Subsequently, the truncated (+)-bornyl diphosphate synthase genes *tSoBPPS*, *tAvBPPS*, *tCbTPS1*, and $tLdBPPS^{S488T}$ were integrated into the chromosomes of ZHY2, respectively. Compared with the chassis strain ZHY2, the strains that included the (+)-bornyl diphosphate synthase genes produced (+)-borneol and also small amounts of monoterpenes (+)-α-pinene, (+)-camphene, (+)-limonene, terpinolene, and β-myrcene (Supporting Information Fig. S3A and S3B). Expression of *tSoBPPS* produced the highest (+)-borneol production of 2.4 mg/L compared with the other three *BPPS* genes (Fig. 2B, Fig. S3C).

Downregulated expression of *ERG20* by replacing its promoter with the *ERG7* promoter significantly improved (+)-borneol production by 423.6% (ZHY3-tSo vs ZHY8, Fig. 2B), suggesting that reducing the GPP consumption by FPP synthesis was essential for (+)-borneol biosynthesis in *S. cerevisiae*. To further increase GPP availability, we overexpressed the mevalonate kinase gene *ERG12* (strain ZHY5), which resulted in a 17.3% increase in (+)-borneol production (Fig. 2B). Dusseaux et al.[19] reported that EfmvaE and EfmvaS catalyze consecutive steps of mevalonate biosynthesis from acetyl-CoA. Overexpression of *EfMvaS* and *EfMvaE* (strain ZHY7) made a small improvement of (+)-borneol production (Fig. 2B). Enhancing GPP availability significantly improved (+)-borneol production but there was a decreased proportion of (+)-borneol among all monoterpenes (Fig. 2B). These results suggested that at high GPP level BPPS was less efficient in biosynthesis of (+)-borneol compared with its by-product monoterpenes. Further overexpression of key genes $HMG2^{K6R}$, *tHMG1*, *ERG8*, *ERG19*, and *IDI1* in ZHY7 resulted in a decrease in (+)-borneol production (Supporting Information Fig. S4).

3.2. Relieving the rate-limiting step of BPP dephosphorylation

Although the production of (+)-borneol increased when we engineered increased availability of GPP precursors, the decrease

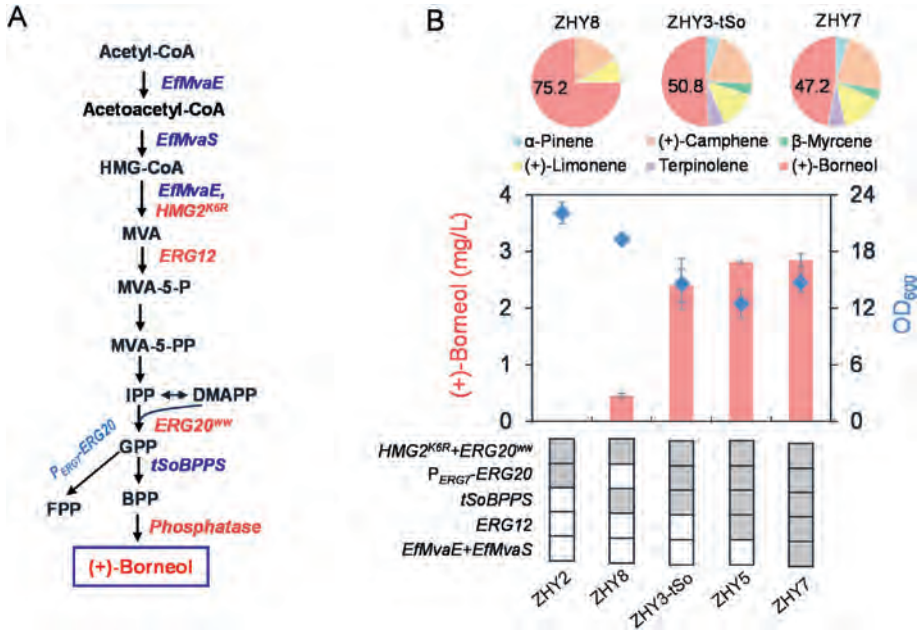

Figure 2 Engineering mevalonate pathway for (+)-borneol production. (A) Schematic of engineering MVA pathway to increase (+)-borneol production. HMG-CoA: 3-hydroxy-3-methylglutaryl-CoA; MVA: mevalonate; MVA-5-P: 5-phosphomevalonate; MVA-5-PP: 5-diphosphomevalonate; IPP: isopentenyl diphosphate; DMAPP: dimethylallyl diphosphate; GPP: geranyl diphosphate; BPP: bornyl diphosphate; FPP: farnesyl diphosphate; *EfMvaE*: acetyl-CoA acetyltransferase/HMG-CoA reductase; *EfMvaS*: HMG-CoA synthase; *HMG2*^{K6R}: HMG-CoA reductase 2 K6R mutant; *ERG12*: mevalonate kinase; *ERG20*: farnesyl diphosphate synthase; *ERG20*^{ww}: farnesyl diphosphate synthase mutant; *tSoBPPS*: truncated bornyl diphosphate synthase. *LPP1*, lipid Phosphate Phosphatase from *Saccharomyces cerevisiae*; *DPP1*, diacylglycerol pyrophosphate (DGPP) phosphatase from *Saccharomyces cerevisiae*. Genes shown in red were overexpressed yeast gene. Genes shown in royal blue were heterologous. Gene shown in blue was downregulated gene. (B) Optimizing the MVA pathway increases (+)-borneol production but decreases (+)-borneol proportion. Data are presented as mean ± SD (n = 3).

of (+)-borneol proportion among the monoterpenes suggested that BPP could not be completely converted into (+)-borneol (Fig. 2B). Unlike the other monoterpenes that can be formed spontaneously by deprotonation or water attack of carbocations in the BPPS catalytic cascade reaction, (+)-borneol biosynthesis requires the removal of a diphosphate group (Fig. S1). We tried to overexpress endogenous diacylglycerol pyrophosphate phosphatases *DPP1* and *LPP1*, which were involved in catalyzing diacylglycerol pyrophosphate to diacylglycerol[48]. It was found that overexpressing *LPP1* or *DPP1* resulted in a 152% and 26% increase in (+)-borneol production, respectively (Fig. 3A). Furthermore, overexpressing *LPP1* and *DPP1* increased the percent of (+)-borneol production, suggesting that BPP dephosphorylation was enhanced. Deletion of *LPP1* and *DPP1* resulted in a decrease of (+)-borneol production (Fig. 3B). Overexpression of other endogenous phosphatases had marginal effects on (+)-borneol production (Supporting Information Fig. S5). These results confirmed that BPP dephosphorylation was a rate-limiting step in (+)-borneol production, and *LPP1* and *DPP1* were involved in (+)-borneol production in *S. cerevisiae*.

The results showed that *LPP1* overexpression was more efficient than overexpression of *DPP1* in increasing (+)-borneol production (Fig. 3A), which might have been due to the different cellular locations of these two phosphatases[48]. Subcellular localization analysis showed that tSoBpps predominantly co-localized with Lpp1 at the Golgi apparatus, which was identified by the Golgi marker protein Sec7[43] (Fig. 3C). Localization of Lpp1 at the Golgi apparatus agreed with reports that Lpp1 is a Golgi membrane protein[48,49]. In contrast, Dpp1 was mainly located on the vacuolar membrane and exhibited limited co-localization with tSoBpps (Fig. 3C). These results explained the superior effect of *LPP1* over *DPP1* in increasing (+)-borneol production and elucidated the Golgi apparatus as the primary site for (+)-borneol production, where *LPP1* catalyzed BPP dephosphorylation into (+)-borneol (Fig. 3D).

Considering the different locations of tSoBpps (Golgi apparatus) and its substrate GPP (cytoplasm, endoplasmic reticulum, and vacuole)[50], we tried to improve their interaction by fusing *tSoBPPS* with the *ERG20*^{ww} gene (high-efficiency GPP synthesis); however, this approach failed to improve (+)-borneol production (ZHY20 vs ZHY67, Fig. 4A). We also tried to improve the interaction between a phosphatase and *tSoBPPS* to facilitate BPP dephosphorylation. A flexible linker (GSG/GGGS), affinity peptides, or cleavable 2A peptides were used as fusion agents; however, all of which failed to improve (+)-borneol production (Supporting Information Fig. S6). Chemical dynamics simulations[51] and Complementary DFT-based molecular dynamics simulations[52] suggested that the active site diphosphate moiety of *tSoBPPS* steers reaction trajectories toward BPP formation (Fig. S1), and increasing the interaction between tSoBpps and Lpp1 might disrupt the stability of the diphosphate moiety and compromised tSoBpps catalytic activity.

3.3. *Optimizing endogenous dephosphorylation pathways*

As BPP dephosphorylation was a rate-limiting step in (+)-borneol production, to further increase the production of (+)-borneol, we increased the copy number of *LPP1* or *DPP1* in the strain ZHY20

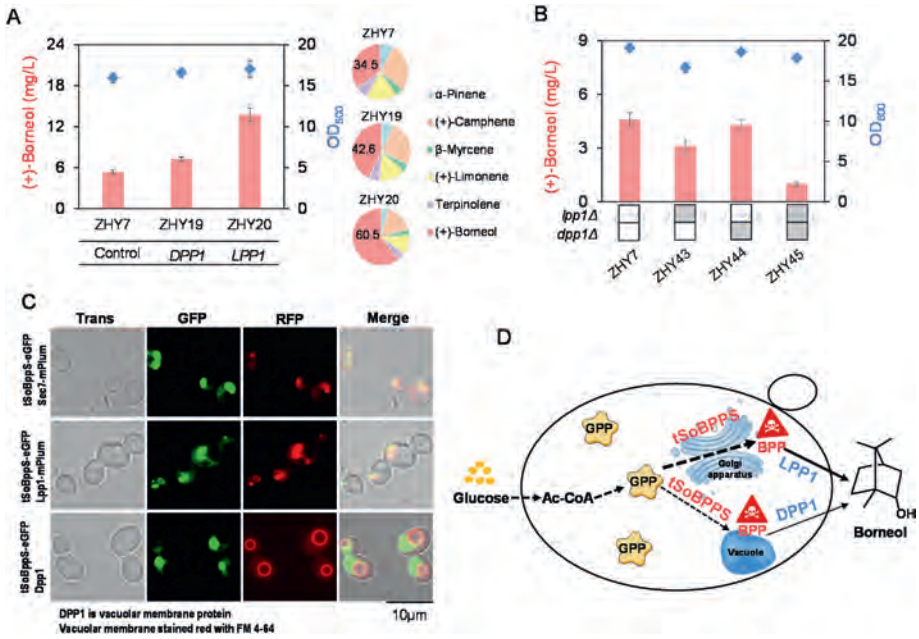

Figure 3 Endogenous phosphatase-mediated (+)-borneol production in *S. cerevisiae*. (A) Overexpressing endogenous phosphatase *LPP1* and *DPP1* increased (+)-borneol production and proportion. (B) Knocking out the endogenous phosphatase *LPP1* and *DPP1* for the production of (+)-borneol. (C) Subcellular localization analysis of tSoBpps, Lpp1, and Dpp1. (D) Schematic diagram of the distribution of *tSoBPPS* and its substrate GPP in yeast. Data are presented as mean ± SD ($n = 3$).

to give strains ZHY61 and ZHY69. However, (+)-borneol production did not increase, and ZHY61 (*LPP1* copy number increase) decreased slightly in growth (Fig. 4B). We then tried to overexpress *LPP1* and *DPP1* simultaneously in strain ZHY20; the resulting strain ZHY73 had a 49.2% higher (+)-borneol production with a slight decrease in growth (Fig. 4A). Similarly, overexpressing *LPP1* and *DPP1* in ZHY67 that possessed the *ERG20*^{ww}-*tSoBPPS* fusion improved (+)-borneol production by 21.4% (ZHY71), with a concomitant decrease in cell growth (Fig. 4A) and cell aggregation (Supporting Information Fig. S7). The compromised cell growth accompanying phosphatase overexpression led us to question whether there was a competitive relationship between (+)-borneol synthesis and cell growth.

In yeast, Lpp1 and Dpp1 are involved in regulating concentrations of diacylglycerol diphosphate, phosphatidate, and diacylglycerol (Fig. 4C), molecules associated with phospholipid metabolism[53-56]. Considering the potential competitive interactions between (+)-borneol synthesis and lipid metabolism, we surmised that the accumulation of (+)-borneol may disrupt lipid metabolism, and, at the same time, lipid metabolism may limit (+)-borneol production (Fig. 4C). Thus, we conducted a lipidomic analysis of strain ZHY7 (borneol production without overexpression of *LPP1/DPP1*) and ZHY73 (borneol production with overexpression of *LPP1/DPP1*). Engineering the mevalonate pathway for borneol production in strain ZHY7 led to a decrease in lipid content compared with the wild-type strain (Fig. 4D), which suggested that high-level BPP biosynthesis competed with endogenous phosphatase and perturbed lipid metabolism. Expression of additional endogenous phosphatases in ZHY73 not only improved (+)-borneol production but also additional endogenous phosphatases restored the lipid content to near wild-type level (Fig. 4D). These results suggested that the biosynthesis of (+)-borneol mediated by endogenous yeast phosphatase occurs at the expense of lipid production, which may explain the limited catalytic efficiency of endogenous phosphatase towards BPP.

3.4. *Heterologous phosphatases boost (+)-borneol production*

Because the catalytic efficiency of endogenous phosphatase toward BPP was limited by lipid metabolism, an increase in endogenous phosphatase copy number posed a risk of retarding cell growth. Therefore, it was necessary to screen for effective heterologous phosphatases. *WvNUDX24* has been reported to be involved in borneol biosynthesis in *Wurfbainia villosa*[37], which unfortunately failed to increase (+)-borneol production in *S. cerevisiae* (Supporting Information Fig. S8). We also tried overexpressing *E. coli* Nudix hydrolase, including *EcNudJ*[22], but that approach resulted in a decrease in (+)-borneol production (Supporting Information Fig. S9). Conversely, overexpressing *tTcNudix1* from *Tanacetum cinerifolium*[57] contributed to an increase in (+)-borneol production without compromising the final cell biomass (Fig. 5A and B). This result showed that a heterologous phosphatase was superior to elevated expression of endogenous phosphatases *LPP1* and *DPP1* (ZHY72 vs ZHY73, Fig. 5B). Co-overexpression of *tTcNudix1* and endogenous *LPP1/DPP1* further boosted (+)-borneol production to 27.3 mg/L (ZHY74, Fig. 5B).

To search for more alternative phosphatases, we analyzed the transcriptome data of two borneol-rich plants, *Cinnamomum camphora* and *Blumea balsamifera*. By evolutionary tree analysis (Fig. 5C), we identified and tested *CcNudix1* and *BbNudix1.3*. It was glad to find that these two genes increased (+)-borneol production by 69% and 31%, respectively (Fig. 5D and E). Notably, sequence comparisons of these Nudix1 genes revealed three short conserved sequences in the center of the protein chains(Supporting Information Fig. S10A), a feature not possessed in other Nudix genes, including *EcNudJ*[22] and *WvNUDX24*[37]. Although other putative Nudix family genes contain the NUDIX domain

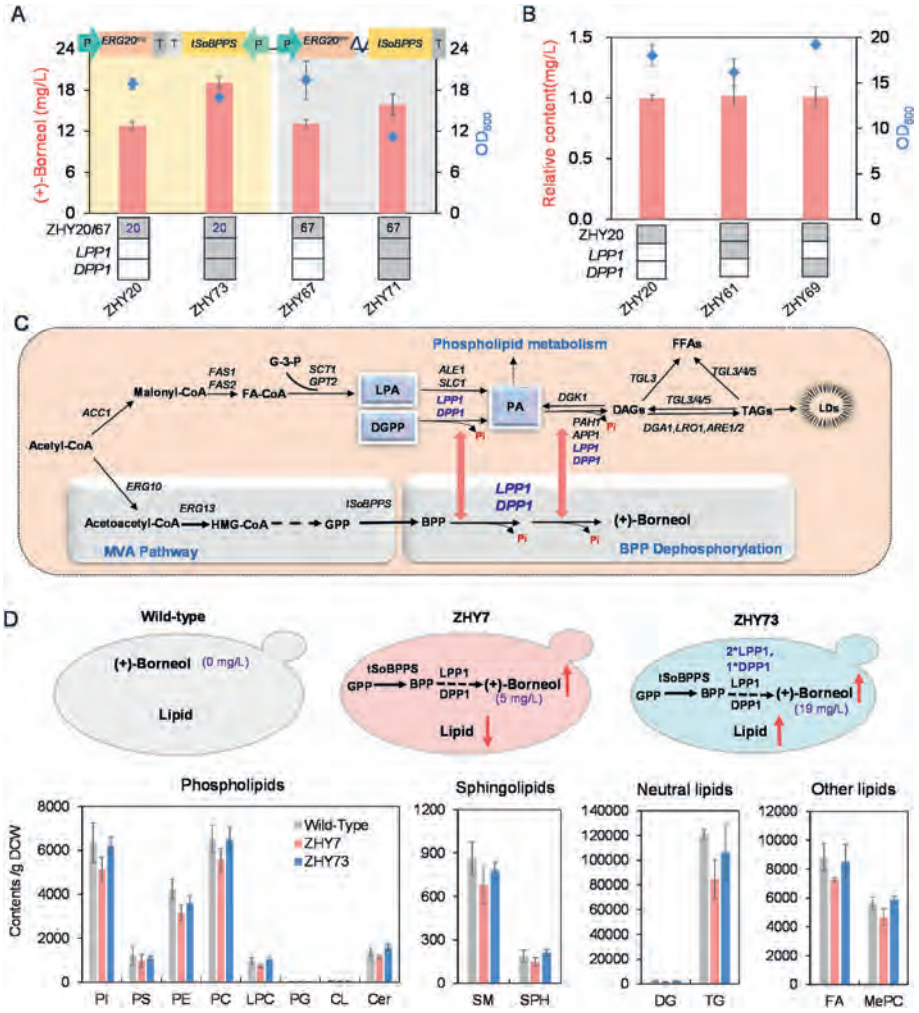

Figure 4 Competition between (+)-borneol synthesis and lipid metabolism. (A) The compromised cell growth accompanying endogenous phosphatase overexpression. (B) The limited catalytic efficiency of endogenous phosphatase towards BPP. (C) Schematic of the competitive relationship between (+)-borneol synthesis and lipid metabolism. DGPP, diacylglycerol diphosphate; PA, phosphatidate; LPA, lysophosphatidic acid; DAG, diacylglycerol; TAG, triacylglycerol; FFA, fatty acid; SE, sterol esters; BPP, bornyl diphosphate; FPP, farnesyl diphosphate. The red double arrows indicate the competitive relationship between (+)-borneol synthesis and lipid metabolism. Genes shown in royal blue were catalytic reactions involving *LPP1* and *DPP1*. (D) Lipid content in wild-type (XC1), the strain without additional endogenous phosphatase (ZHY7), and the strain with additional endogenous phosphatase (ZHY73). PI, phosphatidylinositol; PS, phosphatidylserine; PE, phosphatidylethanolamine; PC, phosphatidylcholine; LPC, lysophosphatidylcholine; PG, phosphatidylglycerol; CL, cardiolipin; Cer, ceramides; SM, sphingomyelin; SPH, sphingosine; DG, diglyceride; TG, triglyceride; FA, fatty acid; Co, coenzyme; MePC, methylphosphatidylcholine. BisMePE, bis-methylphosphatidylethanolamine; dMePE, di-methylphosphatidylethanolamine. Data are presented as mean ± SD ($n = 3$).

(Gx_5Ex_5[UA]xREx_2EExGU, where U is an aliphatic, hydrophobic residue[58]), these genes failed to increase (+)-borneol production (Fig. S10B). These results suggested that Nudix1 hydrolase may have high specificity for BPP in *S. cerevisiae*.

Additionally, we found nine lipid phosphatases grouped in three branches (Fig. 5F). Similar to yeast's *LPP1*, these enzymes exhibited the phosphatase sequence motif present in a superfamily of phosphatase enzymes, comprising three domains: KX_6RP (domain 1), PSGH (domain 2) and SRX_5HX_3D (domain 3)[59-61] (Supporting Information Fig. S11). Overexpressing *C. camphora CcLPPE2*, *CcLPPG*, and *B. balsamifera BbLPPE2* and *BbLPPG* improved (+)-borneol production (Fig. 5G and H), whereas other putative phosphatases failed to promote (+)-borneol biosynthesis in yeast (Supporting Information Fig. S12).

3.5. *Fed-batch fermentation*

To evaluate production potential, we conducted fed-batch fermentation in shake flasks to maximize (+)-borneol production. To avoid supplementation of histidine and uracil during fermentation, we used the *URA3* and *HIS3* prototrophic strain ZHY74UH[62]. Strain ZHY74UH was cultivated in YPD or Delft minimal medium with 20 g/L glucose in the initial batch stage, and YPD or Delft minimal medium was added after all the glucose had been consumed. After 168 h of cultivation in YPD medium, the highest (+)-borneol titer of 753 mg/L with a final OD_{600} of 66 was obtained (Fig. 6A), the highest (+)-borneol titer reported in the literature (Table 1). Growth in Delft minimal medium produced a (+)-borneol titer of 337 mg/L with a final OD_{600} of 59

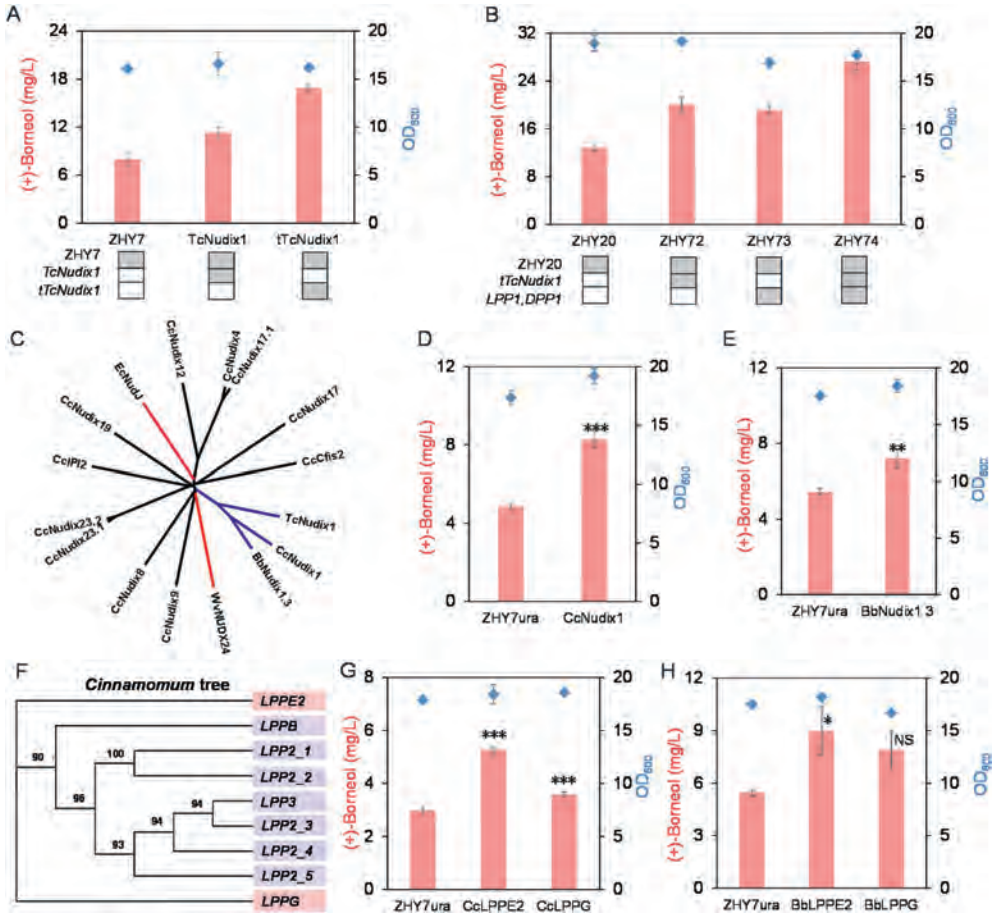

Figure 5 Identification of heterologous phosphatase to improve (+)-borneol production. (A) Effects of *TcNudix1* and *tTcNudix1* on (+)-borneol production. (B) *tTcNudix1* boosting (+)-borneol production. (C) The phylogenetic tree of sixteen Nudix genes. (D) Plasmid expression of *Nudix1* gene of *C. camphora* increased (+)-borneol production. (E) Plasmid expression of *Nudix1* genes of *B. balsamifera* increased (+)-borneol production. (F) Lipid phosphate phosphatase phylogenetic tree of *C. camphora*. (G) Plasmid expression of *LPPE2/LPPG* of *C. camphora* increased (+)-borneol production. (H) Plasmid expression of *LPPE2/LPPG* of *B. balsamifera* increased (+)-borneol production. Data are presented as mean ± SD ($n = 3$). $^{*}P < 0.05$, $^{**}P < 0.01$, $^{***}P < 0.001$. NS, not significant.

(Fig. 6B). After 168 h of cultivation, the (+)-borneol proportion reached 84.7 ± 0.5% and 82.4 ± 0.7% in YPD and Delft minimal medium (Fig. 6C).

4. Discussion

(+)-Borneol is a high-end spice and precious medicine that has been widely used in Chinese medicinal formulae. Here, by metabolic engineering the yeast, we constructed a yeast strain for (+)-borneol production. Enhancing mevalonate flux improved (+)-borneol production and other monoterpenes. We found that BPP dephosphorylation was a bottleneck for (+)-borneol production. We demonstrated that endogenous phosphatases Lpp1 and Dpp1 mediated BPP dephosphorylation to form (+)-borneol, especially, we found that overexpression of LPP1 has the highest production and Lpp1 co-localized with tSoBpps to the Golgi apparatus. To the best of our knowledge, this finding is the first in which the Golgi apparatus was identified as the primary site for terpenoid synthesis. Although the reason for the predominant localization of tSoBpps in the Golgi apparatus is unknown, the phenomenon may be associated with minimizing cell pressure. It was well known that the accumulation of monoterpenes has the potential to cause cell toxicity, whereas using different organelle compartmentalization strategies, such as peroxisome, lipid droplet, and mitochondria[63], can not only improve the catalytic efficiency of enzymes but also avoid the harmful effects of toxic substances on cells. This observation that tSoBpps is located in the Golgi apparatus provides a good case for Golgi apparatus compartmentalization for the production of terpenoids. It will facilitate further investigation on developing the Golgi apparatus as a new organelle for other terpenoid production.

Balancing intracellular dephosphorylation levels is crucial for the synthesis of terpenoids, and *LPP1/DPP1* plays a crucial role in regulating levels of prenyl diphosphate[64]. Previous studies have shown that knocking out *LPP1/DPP1* promotes α-santalene production[25,26]. However, *LPP1* and *DPP1* deletion failed to significantly increase the production of other terpenoids, including monoterpenoids, sesquiterpene, and tetraterpenoids, such as sabinene[47], α-terpinol[65], linalool[66], valencene[67] and α-farnesene[68], β-carotene[69] and lycopene[70]. Interestingly, the effects of *LPP1* and *DPP1* deletion on β-elemene and D-limonene production were opposite in different strains[71,72]. This ambiguous success has misled many researchers to directly knock out LPP1/

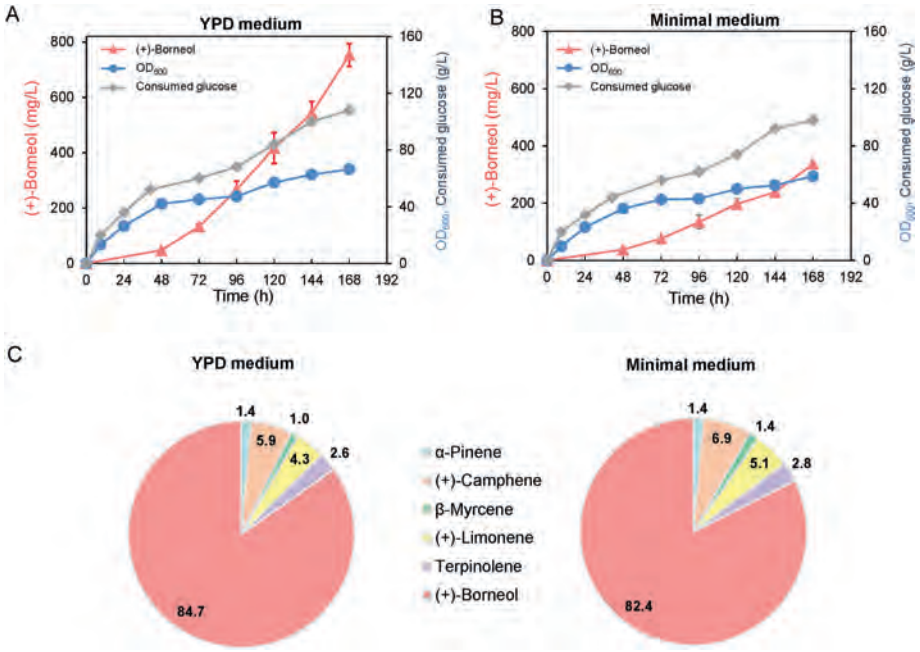

Figure 6 Fed-batch fermentation of prototrophic strain ZHY74UH in shake flasks. YPD (A) or Delft (B) medium was used to culture the strain, and YPD (A) or Delft minimal (B) medium containing 500 g/L glucose was fed after all the glucose had been consumed. (C) The proportion of (+)-borneol in YPD medium and Delft medium at 168 h. Data are presented as mean ± SD ($n = 3$).

DPP1 in the production of terpenoids without sufficient evidence. The Hmg2 degradation rate depended on the level of cellular FPP and the FPP-derived molecule farnesol, thereby mediating early product inhibition of the mevalonate pathway[73]. Therefore, we agree with the statement that deletion of *LPP1* and/or LPP1 positively affects terpenoid synthesis only above a certain threshold level of flux toward FPP[67]. On the one hand, we reduced the flux of FPP by replacing the native *ERG20* promoter with the *ERG7* promoter. It can be conceived that low levels of FPP would not cause feedback inhibition of Hmg2, so the strategies of *LPP1* and *DPP1* deletion were not applicable to our strain. On the other hand, the intermediate BPP, as a prenyl diphosphate, lacks effective exogenous enzymes to channel it towards (+)-borneol, while *LPP1* and *DPP1* account for most of the isoprenoid phosphate phosphatase activities in yeast. Obviously, overexpression of *LPP1*/*DPP1* rather than knockout can effectively balance cell dephosphorylation and promote (+)-borneol synthesis. By analogy to the formation of geranylgeraniol or farnesol via the hydrolysis of GGPP or FPP by *LPP1*/*DPP1*[64], we attributed the production of (+)-borneol to the hydrolysis of BPP by these endogenous phosphatases.

By lipidome analysis, we revealed that this endogenous phosphatase-mediated terpenoid synthesis comes at the expense of lipids, further explaining the importance and complexity of *LPP1* and *DPP1* in terpenoid synthesis and cellular metabolism. Although overexpression of *LPP1* and *DPP1* restored most lipids to their normal levels, this competition imposed significant limitations on the overall (+)-borneol titer and increased copies of *LPP1* and *DPP1* impaired cellular fitness. Therefore, it is imperative to identify heterologous and efficient phosphatases capable of hydrolyzing BPP to facilitate the formation of (+)-borneol. Although Yang et al.[37] showed that *WvNUDX24* is involved in the catalysis of BPP, it failed to increase (+)-borneol production in yeast. In fact, *WvNUDX24* could hydrolyze BPP, GPP, NPP, and FPP to their respective monophosphate products, which may explain its inability to increase (+)-borneol production in engineered strains with high GPP content. After all, the Nudix hydrolases could hydrolyze a wide range of organic pyrophosphates with varying degrees of substrate specificity[58]; this may also result in *EcNudJ* failing to increase (+)-borneol production in yeast. Therefore, we adopted bioinformatics analysis combined with a rapid screening method for BPP-specific phosphatases based on synthetic biology validation and three plant-derived Nudix1 hydrolases (*TcNudix1, CcNudix1*, *BbNudix1.3*) and four lipid phosphatases (*CcLPPE2*, *BbLPPE2*, *CcLPPG*, and *BbLPPG*) were identified. Notably, expressing heterologous phosphatases was feasible to improve (+)-borneol titer without perturbing cellular lipid metabolism, which is superior to elevated expression of endogenous phosphatases. It is noteworthy that the Nudix1 gene is not present in *S. cerevisiae*, and although *YPL117C* (*IDI1*) belongs to the Nudix hydrolase superfamily[58], it failed to improve (+)-borneol production in yeast. Thus, overexpressing t*TcNudix1* satisfied the dual requirement for BPP dephosphorylation and increased (+)-borneol production. This finding that plant-derived Nudix1 hydrolase and lipid phosphatases improve the production of (+)-borneol lays a foundation for further exploration of efficient phosphatase with specific preference for BPP.

BPPS, which converts GPP to BPP, is unusual in that the enzyme incorporates a diphosphate group in its final product, whereas terpene synthase reactions are generally terminated by deprotonation to form alkenes or water-trapping to form alcohols[30-34]. In the case of *SoBPPS*, the anionic diphosphate moiety steers the reaction trajectories toward product formation[51,52], and the final carbocation is quenched by the re-addition of inorganic diphosphate, leading to the production of BPP as the main product[31,35,36] (Fig. S1). Throughout the catalytic process, two conserved motifs, DDxxD and NSE/DTE, contain multiple L-aspartate residues that bind a trinuclear cluster of divalent metal

ions (Mg^{2+}or Mn^{2+}), thereby enabling the complexation of the anionic diphosphate moiety of the substrate[35]. We observed that increasing the interaction between *tSoBPPS* and phosphatase disrupted the stability of the diphosphate moiety and affected the catalytic activity of *tSoBPPS* (Supporting Information Fig. S6). Although dephosphorylation of BPP is a rate-limiting step in (+)-borneol production, it is not feasible to increase (+)-borneol production by assembly of phosphatase into *tSoBPPS*. This finding provides a valuable understanding of the biosynthesis of (+)-borneol, highlighting the importance of the balance between BPP formation and dephosphorylation in a consecutive manner. Therefore, further enhancement of the dephosphorylation pathway by expression of highly efficient and BPP-specific phosphatase is a feasible strategy to increase the production and proportion of (+)-borneol.

5. Conclusions

Microbes have been extensively harnessed for the high-level production of various terpenoids by engineering isoprenoid synthase, biosynthesis pathways, and cell metabolism. However, the dephosphorylation of isoprenoid synthase has largely been ignored, potentially contributing to the low production of (+)-borneol in yeast. In this study, we systematically identified and characterized phosphatases involved in BPP dephosphorylation and optimized the cellular dephosphorylation process by overexpressing endogenous phosphatase and balancing cellular dephosphorylation metabolism, which significantly improved (+)-borneol production. In summary, we successfully reprogrammed the metabolism of *S. cerevisiae* to achieve high-level production of (+)-borneol by engineering BPP dephosphorylation and the mevalonate pathway. This novel dephosphorylation engineering strategy should pave a new way for enhancing isoprenoid biosynthesis in microbial cell factories.

Acknowledgments

This work was supported by National Key R&D Program of China (2020YFA0908000), the CACMS Innovation Fund (CI2021A04109, CI2023D002, China), Key project at central government level: the ability to establish sustainable use of valuable Chinese Medicine Resources (2060302, China).

Author contributions

Haiyan Zhang: Writing − original draft, Visualization, Investigation, Data curation. Peng Cai: Methodology. Juan Guo: Supervision. Jiaoqi Gao: Methodology. Linfeng Xie: Methodology. Ping Su: Methodology. Xiaoxin Zhai: Software. Baolong Jin: Methodology. Guanghong Cui: Writing − review & editing, Validation. Yongjin J. Zhou: Writing − review & editing. Luqi Huang: Project administration.

Conflicts of interest

The authors have no conflicts of interest to declare.

Appendix A. Supporting information

Supporting information to this article can be found online at https://doi.org/10.1016/j.apsb.2024.12.039.

References

1. Granger RE, Campbell EL, Johnston GA. (+)- and (−)-borneol: efficacious positive modulators of GABA action at human recombinant $\alpha_1\beta_2\gamma_{2L}$ $GABA_A$ receptors. *Biochem Pharmacol* 2005; **69**:1101−11.
2. Chen L, Su J, Li L, Li B, Li W. A new source of natural D-borneol and its characteristic. *J Med Plants Res* 2011;**5**:3440−7.
3. Cai Z, Lei XL, Lin ZF, Zhao J, Wu FZ, Yang ZX, et al. Preparation and evaluation of sustained-release solid dispersions co-loading gastrodin with borneol as an oral brain-targeting enhancer. *Acta Pharm Sin B* 2014;**4**:86−93.
4. Zou L, Zhang Y, Li W, Zhang JM, Wang D, Fu J, et al. Comparison of chemical profiles, anti-inflammatory activity, and UPLC-Q-TOF/MS-based metabolomics in endotoxic fever rats between synthetic borneol and natural borneol. *Molecules* 2017; **22**:1446.
5. Xin Y, Zhao HJ, Xu JQ, Xie ZX, Li GF, Gan ZH, et al. Borneol-modified chitosan: antimicrobial adhesion properties and application in skin flora protection. *Carbohydr Polym* 2020;**228**: 115378.
6. Ji J, Zhang RH, Li HM, Zhu J, Pan YZ, Guo Q. Analgesic and anti-inflammatory effects and mechanism of action of borneol on photodynamic therapy of acne. *Environ Toxicol Pharmacol* 2020;**75**: 103329.
7. Liu SY, Long Y, Yu S, Zhang DK, Yang QY, Ci ZM, et al. Borneol in cardio-cerebrovascular diseases: pharmacological actions, mechanisms, and therapeutics. *Pharmacol Res* 2021;**169**:105627.
8. Ouyang SL, Long GY, Huang LQ, Xiang HY. New resources of natural borneol. *Jiangxi For Sci Technology* 2005;**5**:38.
9. Zhang YS, Wang CZ, Zhou H, Chen HX, Ye JZ, Tao R. Chemical components of volatile oil in *Cinnamomum camphora* chvar borneol leaf from different Habitats by GC−MS. *Chin J Exp Traditional Med Formulae* 2014;**20**:57−61.
10. Lu Y, Du SY, Yao ZL, Zhao PY, Zhai YS. Study on natural borneol and synthetic borneol affecting mucosal permeability of gardenia extract. *China J Chin Mater Med* 2009;**34**:1207−10.
11. Paddon CJ, Westfall PJ, Pitera DJ, Benjamin K, Fisher K, McPhee D, et al. High-level semi-synthetic production of the potent antimalarial artemisinin. *Nature* 2013;**496**:528−32.
12. Luo XZ, Reiter MA, d'Espaux L, Wong J, Denby CM, Lechner A, et al. Complete biosynthesis of cannabinoids and their unnatural analogues in yeast. *Nature* 2019;**567**:123−6.
13. Zhang J, Hansen LG, Gudich O, Viehrig K, Lassen LMM, Schrübbers L, et al. A microbial supply chain for production of the anti-cancer drug vinblastine. *Nature* 2022;**609**:341−7.
14. Galanie S, Thodey K, Trenchard IJ, Filsinger Interrante M, Smolke CD. Complete biosynthesis of opioids in yeast. *Science* 2015;**349**:1095−100.
15. Zhu K, Kong J, Zhao BX, Rong LX, Liu SQ, Lu ZH, et al. Metabolic engineering of microbes for monoterpenoid production. *Biotechnol Adv* 2021;**53**:107837.
16. Cao X, Yu W, Chen Y, Yang S, Zhao ZB, Nielsen J, et al. Engineering yeast for high-level production of diterpenoid sclareol. *Metab Eng* 2023;**75**:19−28.
17. Liu CL, Xue K, Yang YK, Liu XX, Li Y, Lee TS, et al. Metabolic engineering strategies for sesquiterpene production in microorganism. *Crit Rev Biotechnol* 2022;**42**:73−92.
18. Zhang L, Xiao WH, Wang Y, Yao MD, Jiang GZ, Zeng BX, et al. Chassis and key enzymes engineering for monoterpenes production. *Biotechnol Adv* 2017;**35**:1022−31.
19. Dusséaux S, Wajn WT, Liu YX, Ignea C, Kampranis SC. Transforming yeast peroxisomes into microfactories for the efficient production of high-value isoprenoids. *Proc Natl Acad Sci U S A* 2020;**117**:31789−99.
20. Jiang GZ, Yao MD, Wang Y, Zhou L, Song TQ, Liu H, et al. Manipulation of GES and ERG20 for geraniol overproduction in & *Saccharomyces cerevisiae*. *Metab Eng* 2017;**41**:57−66.

21. Li RS, Wang K, Wang D, Xu LP, Shi YS, Dai ZB, et al. Production of plant volatile terpenoids (rose oil) by yeast cell factories. *Green Chem* 2021;**23**:5088−96.
22. Lei DW, Qiu ZT, Wu JH, Qiao B, Qiao JJ, Zhao GR. Combining Metabolic and Monoterpene Synthase Engineering for de Novo Production of Monoterpene Alcohols in *Escherichia coli*. *ACS Synth Biol* 2021;**10**:1531−44.
23. Ma R, Su P, Guo J, Jin BL, Ma Q, Zhang HY, et al. Bornyl diphosphate synthase from *Cinnamomum burmanni* and its application for (+)-borneol biosynthesis in yeast. *Front Bioeng Biotechnol* 2021;**9**: 631863.
24. Ma R, Su P, Ma Q, Guo J, Chen SQ, Jin BL, et al. Identification of (−)-bornyl diphosphate synthase from *Blumea balsamifera* and its application for (−)-borneol biosynthesis in *Saccharomyces cerevisiae*. *Synth Syst Biotechnol* 2021;**7**:490−7.
25. Scalcinati G, Partow S, Siewers V, Schalk M, Daviet L, Nielsen J. Combined metabolic engineering of precursor and co-factor supply to increase α-santalene production by *Saccharomyces cerevisiae*. *Microb Cell Fact* 2012;**11**:117.
26. Scalcinati G, Knuf C, Partow S, Chen Y, Maury J, Schalk M, et al. Dynamic control of gene expression in *Saccharomyces cerevisiae* engineered for the production of plant sesquitepene α-santalene in a fed-batch mode. *Metab Eng* 2012;**14**:91−103.
27. Tokuhiro K, Muramatsu M, Ohto C, Kawaguchi T, Obata S, Muramoto N, et al. Overproduction of geranylgeraniol by metabolically engineered *Saccharomyces cerevisiae*. *Appl Environ Microbiol* 2009;**75**:5536−43.
28. Cardoza RE, McCormick SP, Lindo L, Mayo-Prieto S, González-Cazón D, Martínez-Reyes N, et al. Effect of farnesol in *Trichoderma* physiology and in fungal−plant interaction. *J Fungi (Basel)* 2022;**8**: 1266.
29. Cheng YT, Luo LL, Tang H, Wang J, Ren L, Cui GH, et al. Engineering the microenvironment of P450s to enhance the production of diterpenoids in *Saccharomyces cerevisiae*. *Acta Pharm Sin B* 2024;**14**: 4608−18.
30. Hong YJ, Tantillo DJ. Quantum chemical dissection of the classic terpinyl/pinyl/bornyl/camphyl cation conundrum—the role of pyrophosphate in manipulating pathways to monoterpenes. *Org Biomol Chem* 2010;**8**:4589−600.
31. Wise ML, Savage TJ, Katahira E, Croteau R. Monoterpene synthases from common sage (*Salvia officinalis*). cDNA isolation, characterization, and functional expression of (+)-sabinene synthase, 1,8-cineole synthase, and (+)-bornyl diphosphate synthase. *J Biol Chem* 1998;**273**:14891−9.
32. Schwab W, Williams DC, Davis EM, Croteau R. Mechanism of monoterpene cyclization: stereochemical aspects of the transformation of noncyclizable substrate analogs by recombinant (−)-limonene synthase, (+)-bornyl diphosphate synthase, and (−)-pinene synthase. *Arch Biochem Biophys* 2001;**392**:123−36.
33. Whittington DA, Wise ML, Urbansky M, Coates RM, Croteau RB, Christianson DW. Bornyl diphosphate synthase: structure and strategy for carbocation manipulation by a terpenoid cyclase. *Proc Natl Acad Sci U S A* 2002;**99**:15375−80.
34. Christianson DW. Structural biology and chemistry of the terpenoid cyclases. *Chem Rev* 2006;**106**:3412−42.
35. Kim H, Srividya N, Lange I, Huchala EW, Ginovska B, Lange BM, et al. Determinants of selectivity for the formation of monocyclic and bicyclic products in monoterpene synthases. *ACS Catal* 2022;**12**:7453−69.
36. Wise ML, Pyun HJ, Helms G, Assink B, Coates RM, Croteau RB. Stereochemical disposition of the geminal dimethyl groups in the enzymatic cyclization of geranyl diphosphate to (+)-bornyl diphosphate by recombinant (+)-bornyl diphosphate synthase from *Salvia officinalis*. *Tetrahedron* 2001;**57**:5327−34.
37. Yang P, Chen YX, Wang TT, Huang XS, Zhan RT, Yang JF, et al. Nudix hydrolase *WvNUDX24* is involved in borneol biosynthesis in *Wurfbainia villosa*. *Plant J* 2024;**118**:1218−31.
38. Gietz RD, Schiestl RH. High-efficiency yeast transformation using the LiAc/SS carrier DNA/PEG method. *Nat Protoc* 2007;**2**:31−4.
39. Kong SJ, Yu W, Gao N, Zhai XX, Zhou YJ. Expanding the neutral sites for integrated gene expression in *Saccharomyces cerevisiae*. *FEMS Microbiol Lett* 2022;**369**:fnac081.
40. Mans R, van Rossum HM, Wijsman M, Backx A, Kuijpers NG, van den Broek M, et al. CRISPR/Cas9: a molecular Swiss army knife for simultaneous introduction of multiple genetic modifications in *Saccharomyces cerevisiae*. *FEMS Yeast Res* 2015;**15**:fov004.
41. Yang S, Cao X, Yu W, Li SY, Zhou YJ. Efficient targeted mutation of genomic essential genes in yeast *Saccharomyces cerevisiae*. *Appl Microbiol Biotechnol* 2020;**104**:3037−47.
42. Zhou YJ, Gao W, Rong QX, Jin GJ, Chu HY, Liu WJ, et al. Modular pathway engineering of diterpenoid synthases and the mevalonic acid pathway for miltiradiene production. *J Am Chem Soc* 2012;**134**: 3234−41.
43. Zhu J, Zhang ZT, Tang SW, Zhao BS, Li H, Song JZ, et al. A validated set of fluorescent-protein-based markers for major organelles in yeast (*Saccharomyces cerevisiae*). *mBio* 2019;**10**:e01691-19.
44. Xuan QH, Hu CX, Yu D, Wang LC, Zhou Y, Zhao XJ, et al. Development of a high coverage pseudotargeted lipidomics method based on ultra-high performance liquid chromatography−mass spectrometry. *Anal Chem* 2018;**90**:7608−16.
45. Ignea C, Raadam MH, Motawia MS, Makris AM, Kampranis SC. Orthogonal monoterpenoid biosynthesis in yeast constructed on an isomeric substrate. *Nat Commun* 2019;**10**:3799.
46. Ignea C, Trikka FA, Kourtzelis I, Argiriou A, Kanellis AK, Kampranis SC, et al. Positive genetic interactors of HMG2 identify a new set of genetic perturbations for improving sesquiterpene production in *Saccharomyces cerevisiae*. *Microb Cell Fact* 2012;**11**:162−77.
47. Ignea C, Pontini M, Maffei ME, Makris AM, Kampranis SC. Engineering monoterpene production in yeast using a synthetic dominant negative geranyl diphosphate synthase. *ACS Synth Biol* 2014;**3**: 298−306.
48. Carman GM. Discoveries of the phosphatidate phosphatase genes in yeast published in the Journal of Biological Chemistry. *J Biol Chem* 2019;**294**:1681−9.
49. Huh WK, Falvo JV, Gerke LC, Carroll AS, Howson RW, Weissman JS, et al. Global analysis of protein localization in budding yeast. *Nature* 2003;**425**:686−91.
50. Coudert E, Gehant S, de Castro E, Pozzato M, Baratin D, Neto T, et al. Annotation of biologically relevant ligands in UniProtKB using ChEBI. *Bioinformatics* 2023;**39**:btac793.
51. Major DT, Weitman M. Electrostatically guided dynamics—the root of fidelity in a promiscuous terpene synthase?. *J Am Chem Soc* 2012; **134**:19454−62.
52. Weitman M, Major DT. Challenges posed to bornyl diphosphate synthase: diverging reaction mechanisms in monoterpenes. *J Am Chem Soc* 2010;**132**:6349−60.
53. Loewen CJR, Gaspar ML, Jesch SA, Delon C, Ktistaki NT, Henry SA, et al. Phospholipid metabolism regulated by a transcription factor sensing phosphatidic acid. *Science* 2004;**304**:1644−7.
54. Carman GM, Henry SA. Phosphatidic acid plays a central role in the transcriptional regulation of glycerophospholipid synthesis in *Saccharomyces cerevisiae*. *J Biol Chem* 2007;**282**:37293−7.
55. Carman GM, Han GS. Phosphatidic acid phosphatase, a key enzyme in the regulation of lipid synthesis. *J Biol Chem* 2009;**284**:2593−7.
56. Wu WI, Liu YS, Riedel B, Wissing JB, Fischl AS, Carman GM. Purification and characterization of diacylglycerol pyrophosphate phosphatase from *Saccharomyces cerevisiae*. *J Biol Chem* 1996;**271**: 1868−76.
57. Li W, Lybrand DB, Xu HY, Zhou F, Last RL, Pichersky E. A trichome-specific, plastid-localized *Tanacetum cinerariifolium* nudix protein hydrolyzes the natural pyrethrin pesticide biosynthetic intermediate trans-chrysanthemyl diphosphate. *Front Plant Sci* 2020;**11**:482.
58. McLennan AG. The Nudix hydrolase superfamily. *Cell Mol Life Sci* 2006;**63**:123−43.
59. Neuwald AF. An unexpected structural relationship between integral membrane phosphatases and soluble haloperoxidases. *Protein Sci* 1997;**6**:1764−7.

60. Hemrika W, Renirie R, Dekker HL, Barnett P, Wever R. From phosphatases to vanadium peroxidases: a similar architecture of the active site. *Proc Natl Acad Sci U S A* 1997;**94**: 2145−9.
61. Stukey J, Carman GM. Identification of a novel phosphatase sequence motif. *Protein Sci* 1997;**6**:469−72.
62. Yan CX, Gao N, Cao X, Yao L, Zhou YJ, Gao JQ. Auxotrophs compromise cell growth and fatty acid production in *Saccharomyces cerevisiae*. *Biotechnol J* 2023;**18**:e2200510.
63. Jin K, Xia HZ, Liu YF, Li JH, Du GC, Lv XQ, et al. Compartmentalization and transporter engineering strategies for terpenoid synthesis. *Microb Cell Fact* 2022;**21**:92.
64. Faulkner A, Chen X, Rush J, Horazdovsky B, Waechter CJ, Carman GM, et al. The LPP1 and DPP1 gene products account for most of the isoprenoid phosphate phosphatase activities in *Saccharomyces cerevisiae*. *J Biol Chem* 1999;**274**: 14831−7.
65. Zhang C, Li M, Zhao GR, Lu W. Alpha-Terpineol production from an engineered *Saccharomyces cerevisiae* cell factory. *Microb Cell Fact* 2019;**18**:160.
66. Zhang YY, Cao XS, Wang J, Tang F. Enhancement of linalool production in *Saccharomyces cerevisiae* by utilizing isopentenol utilization pathway. *Microb Cell Fact* 2022;**21**:212.
67. Farhi M, Marhevka E, Masci T, Marcos E, Eyal Y, Ovadis M, et al. Harnessing yeast subcellular compartments for the production of plant terpenoids. *Metab Eng* 2011;**13**:474−81.
68. Wang JH, Jiang W, Liang CJ, Zhu LH, Li YR, Mo Q, et al. Overproduction of α-farnesene in *Saccharomyces cerevisiae* by farnesene synthase screening and metabolic engineering. *J Agric Food Chem* 2021;**69**:3103−13.
69. Zhao YJ, Zhang YP, Nielsen J, Liu ZH. Production of β-carotene in *Saccharomyces cerevisiae* through altering yeast lipid metabolism. *Biotechnol Bioeng* 2021;**118**:2043−52.
70. Zhang XY, Chen ST, Lin Y, Li WJ, Wang DG, Ruan SP, et al. Metabolic engineering of *Pichia pastoris* for high-level production of lycopene. *ACS Synth Biol* 2023;**12**:2961−72.
71. Bröker JN, Müller B, Prüfer D, Schulze Gronover C. Combinatorial metabolic engineering in *Saccharomyces cerevisiae* for the enhanced production of the FPP-derived sesquiterpene germacrene. *Bioeng (Basel)* 2020;**7**:135.
72. Hu ZH, Li HX, Weng YR, Li P, Zhang CY, Xiao DG. Improve the production of D-limonene by regulating the mevalonate pathway of *Saccharomyces cerevisiae* during alcoholic beverage fermentation. *J Ind Microbiol Biotechnol* 2020;**47**:1083−97.
73. Shearer AG, Hampton RY. Lipid-mediated, reversible misfolding of a sterol-sensing domain protein. *EMBO J* 2005;**24**:149−59.